arXiv:1408.4183v1 [physics.data-an] 19 Aug 2014

Identifying transitions in finite systems by means of partition function zeros and microcanonical inflection-point analysis: A comparison for elastic flexible polymers

Julio C. S. Rocha,[1,*] Stefan Schnabel,[2,†] David P. Landau,[1,‡] and Michael Bachmann[1,3,4,§]

[1] *Center for Simulational Physics, The University of Georgia, Athens, Georgia 30602, USA*
[2] *Institut für Theoretische Physik and Centre for Theoretical Sciences (NTZ), Universität Leipzig, Postfach 100920, D-04009 Leipzig, Germany*
[3] *Instituto de Física, Universidade Federal de Mato Grosso, Cuiabá (MT), Brazil*
[4] *Departamento de Física, Universidade Federal de Minas Gerais, Belo Horizonte (MG), Brazil*

(Dated: August 20, 2014)

For the estimation of transition points of finite elastic, flexible polymers with chain lengths from 13 to 309 monomers, we compare systematically transition temperatures obtained by the Fisher partition function zeros approach with recent results from microcanonical inflection-point analysis. These methods rely on accurate numerical estimates of the density of states, which have been obtained by advanced multicanonical Monte Carlo sampling techniques. Both the Fisher zeros method and microcanonical inflection-point analysis yield very similar results and enable the unique identification of transition points in finite systems, which is typically impossible in the conventional canonical analysis of thermodynamic quantities.

PACS numbers: 05.10.-a,05.70.Fh,82.35.Lr

I. INTRODUCTION

Phase transitions are among the most fascinating phenomena in nature and huge efforts have been made to understand the features that characterize these cooperative processes for many different systems in a general and systematic way. Strictly speaking, thermodynamic phase transitions occur only in the thermodynamic limit, i.e., for infinitely large systems. However, recent growing interest has also involved finite systems. Prominent representatives for such systems are finite polymer chains and, in particular, proteins. Because of surprisingly manifest common properties of transitions in finite and infinite systems, the question arose to what extent the relationship between "pseudo-transitions" in finite systems and their infinite-system counterparts can be stressed. It is well known that the precise determination of the location of transitions in finite systems is typically ambiguous and different fluctuating quantities suggest different points in parameter space as transition points. In the thermodynamic limit, scale freedom would let this space collapse to a single unique transition point. However, most contemporary problems in soft condensed matter and technology are apparently of small size, for which the thermodynamic limit is not applicable at all. For this reason, it is necessary to verify if the methods of statistical analysis that have been developed for infinitely large systems and have proven to be so extremely successful in these cases can be employed for, or adapted to, finite systems as well.

Another important aspect is the fact that computer simulations open a completely new view on statistical physics, as only the most recently developed computational methods and algorithms enable the accurate study of fundamental statistical quantities that could hardly be approached by theoretical methods in the course of the establishment of the theory of complex phenomena and phase transitions in the past decades. One such quantity is the density of states $g(E)$, i.e., the number of system configurations within a given energy interval. Its logarithm can be associated with the entropy of the system in energy space, $S(E) = k_{\mathrm{B}} \ln g(E)$, and the first derivative with respect to energy yields the inverse temperature $\beta(E) = dS(E)/dE$. It has been shown recently that the careful analysis of inflection points of this quantity reveals all transitions in the system uniquely and without any ambiguity [1]. Since in this approach the temperature is considered to be a derived quantity and a function of energy, this method is a representative of microcanonical statistical analysis.

In this paper, we will also make use of the density of states, but we are going to interpret its features in a canonical way by considering the partition function $Z(T)$ of the system as a function of the (canonical) temperature T. The thermodynamic potential associated with the canonical ensemble (we consider fixed system size N and volume V) is the free energy $F(T) = -k_{\mathrm{B}} T \ln Z(T)$. Thermodynamic phase transitions are located in temperature space, where a derivative of F of a certain order exhibits a singularity [2–6]. Examples are the canonical entropy $S(T) = -(dF(T)/dT)_{N,V}$ and response quantities such as the heat capacity $C_V = T(dS(T)/dT)_{N,V} = -T(d^2F(T)/dT^2)_{N,V}$. Yang and Lee were the first to relate catastrophic singularities to partition function zeros in the grand canonical ensemble by introducing complex fugacities [7]. Fisher evolved this idea for the canonical

* E-mail: jcsrocha@physast.uga.edu
† E-mail: stefan.schnabel@itp.uni-leipzig.de
‡ E-mail: dlandau@hal.physast.uga.edu; Homepage: http://www.csp.uga.edu
§ E-mail: bachmann@smsyslab.org; Homepage: http://www.smsyslab.org

partition function by introducing a complex temperature plane [8].

There is extensive literature on applications of such methods to various physical systems such as spin models (see, e.g., Refs. [9–11]), proteins [12, 13], and to polymers [14, 15]. Most applications of the partition function zero analysis method are considered to be alternative approaches to scaling properties near phase transitions in large systems. However, this method is also promising for the identification and characterization of analogs of phase transitions in finite systems, in particular in finite linear polymer chains that are known to exhibit a variety of structural transitions which sensitively depend on the chain length [1, 16–18]. The understanding of these structure formation processes is relevant from both fundamental scientific and applied technological perspectives of molecular building-block systems.

Typically these processes are accompanied by nucleation transitions, where crystalline shapes form from a liquid or vapor phase. Crystalline or glass-like structures of single polymer chains can serve as the basic elements of larger assemblies on nanoscopic scales; and beyond that, the crystallization behavior exhibits strong similarities to the cluster formation of colloidal (or atomic) particles [17]. The nucleation is governed by finite-size and surface effects, where functionalization is based on the individual structural properties of small molecules forming large-scale composites [17]. These effects can be analyzed by means of microcanonical thermodynamics [19], in which case transition properties can be derived directly and systematically from the caloric entropy curve [1]. This approach has been successfully applied to a variety of structural transitions in macromolecular systems such as folding [1, 20–22], aggregation [23], and adsorption processes of polymers and proteins [24, 25]. One particular problem that has gained increased interest recently is the influence of the interaction range on the stability of structural phases [21, 26]. This has been addressed by means of systematic microcanonical analyses in discrete and continuous polymer models.

In principle, once the density of states $g(E)$ is given, the partition function can easily be calculated and its zeros identified. However, examples of systems for which $g(E)$ can be calculated exactly, or quite accurately by theoretical methods, are very rare. It requires sophisticated numerical methods such as generalized-ensemble Monte Carlo sampling that allow for accurate estimates of $g(E)$. Among the most popular methods are multicanonical sampling [27, 28] and the Wang-Landau method [29]. These methods are capable of scanning the entire phase space effectively in a single simulation.

Compared to recent studies on partition function zero analyses of polymers such as Ref. [14], we here employ a more realistic coarse-grained model for elastic, flexible polymers with continuous, distance-dependent monomer-monomer interactions based on van der Waals forces. Recently developed sophisticated simulation methodologies specific to this model [30] enable a very precise estimation of fundamental statistical quantities such as the density of states. This is essential for the careful identification of low-entropy phases that include liquid-solid and solid-solid transitions. For finite systems, these transitions are strongly affected by finite-size effects, which are of particular interest in this comparative study of advanced statistical analysis methods. One major question is whether the partition function zeros method, which is effectively a canonical approach, is capable of revealing the same intricate details of these effects as the microcanonical inflection-point analysis [1]. For this purpose, we systematically analyze the canonical partition function zeros for all chain lengths ranging from 13 to 309 monomers in this model and identify and classify all structural transitions. Since the finite-size effects in the solid phases are surface effects specific to the explicit chain length, transitions in between them do not exhibit obvious scaling properties [1, 17, 31]. Therefore, scaling considerations are not in the focus of this study.

This paper is organized as follows: In Sec. II, we review the partition function zeros approach and describe the numerical methods used for the estimation of the density of states and for the identification of the Fisher zeros. This section also includes a brief discussion of the microcanonical inflection-point analysis. The results of our study are presented in Sec. III, where we first discuss the different scenarios in the liquid-solid and solid-solid transition regimes thoroughly by investigating the zero maps for four representative examples that differ in the processes of Mackay and anti-Mackay overlayer formation. We then generalize and summarize the results obtained by the zeros method for all polymers with chain lengths up to 309 monomers and compare with former results obtained by microcanonical inflection-point analysis [1]. The paper is concluded by a summary in Sec. IV.

II. METHODS AND MODEL

A. Partition function zeros and thermodynamics

We consider a polymer system in thermal equilibrium with a heat bath that is described by the canonical NVT ensemble (constant particle number N, volume V, and temperature T). This ensemble connects microscopic quantities and thermodynamical properties via statistical relations described by the canonical partition function Z. In thermal equilibrium, the probability for a discrete energetic state is $p_m = g_m e^{-\beta E_m}/Z$, where g_m denotes the density of states at each energy E_m; $\beta = 1/k_{\rm B}T$ is the inverse thermal energy and $k_{\rm B}$ is the Boltzmann constant. In this work the units are chosen so that $k_{\rm B} = 1$. For a discrete ensemble of energetic states, the partition function reads

$$Z = \sum_m g_m e^{-\beta E_m} = e^{-\beta E_0} \sum_m g_m e^{-\beta(E_m - E_0)}, \qquad (1)$$

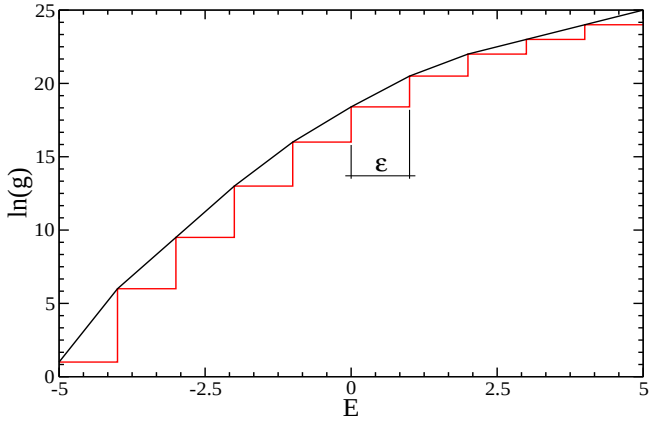

FIG. 1. Pictorial demonstration of the discretization of a continuous density of states over an energy range which is divided in n bins of size ε. Here the bins are labeled from 0 to $n-1$, thus the energy of the mth bin is $E_m = E_0 + m\varepsilon$. All states with energy between E_m and $E_m + \varepsilon$ are recorded in the mth bin g_m.

where we have extracted the Boltzmann factor of the ground state for future convenience. All essential thermodynamic quantities such as entropy and response functions like the heat capacity derive from the free energy $F = -\ln Z/\beta$.

For the subsequent analysis of a model with a continuous energy spectrum, it is necessary to discretize the density of states. Estimates obtained by means of generalized-ensemble Monte Carlo methods such as multicanonical [27, 28] and Wang-Landau sampling [29] are naturally discrete in energy space (see Fig. 1). If the energy bin size is chosen to be ε, the partition function (1) can be rewritten as

$$Z = e^{-\beta E_0} \sum_{m=0}^{n-1} g_m e^{-\beta m\varepsilon}, \tag{2}$$

where n denotes the total number of bins.

Defining $x \equiv e^{-\beta\varepsilon}$, the partition function can assume the form of a polynomial

$$Z = e^{-\beta E_0} \sum_{m=0}^{n-1} g_m x^m = e^{-\beta E_0} \prod_{j=1}^{n-1} (x - x_j). \tag{3}$$

In the latter expression, the polynomial was decomposed into linear factors $(x - x_j)$, where x_j denotes the jth zero (or root) of the polynomial. With the polynomial defined in this way, the density of states can cover the entire space of energy for both positive and negative energies. Note that $x \geq 0$; if $T \to 0$ then $x \to 0$, whereas $x \to 1$, if $T \to \infty$.

In Eq. (3), Z is written as a polynomial of degree $n-1$ which has $n-1$, generally complex, roots. Since $Z \in \Re$ and for a finite system always $Z > 0$ and since the coefficients g_m are nonzero positive real numbers, the roots must occur as complex conjugate pairs $a_j \pm ib_j$ with $a, b \in \Re$. Real-valued roots must be negative.

Once the partition function is determined thermodynamic quantities can be extracted from the the Helmholtz free energy F. The internal energy is

$$U = \langle E \rangle = -\frac{\partial \ln Z}{\partial \beta} \tag{4}$$

and, most interesting for the following consideration, the specific heat at constant volume reads

$$c_V = \frac{1}{N} \left(\frac{\partial U}{\partial T} \right)_V = \frac{k_B \beta^2}{N} \frac{\partial^2 \ln Z}{\partial \beta^2}. \tag{5}$$

Inserting the factorization (3), these quantities can also be expressed by the Fisher zero components:

$$U = E_0 + \sum_{j=1}^{n-1} \left(\frac{\varepsilon x}{x - x_j} \right) = E_0 + \sum_{j=1}^{n-1} \left(\frac{\varepsilon x (x - a_j)}{(x - a_j)^2 + b_j^2} \right), \tag{6}$$

and

$$\begin{aligned} c_V &= \frac{k_B x (\ln x)^2}{N} \sum_{j=1}^{n-1} \left(\frac{-x_j}{(x - x_j)^2} \right) \\ &= \frac{k_B x (\ln x)^2}{N} \sum_{j=1}^{n-1} \left(\frac{-a_j (x - a_j)^2 + b_j^2 (2x - a_j)}{[(x - a_j)^2 + b_j^2]^2} \right). \end{aligned} \tag{7}$$

Obviously, this expression can only become singular at $x = a_j$, if $b_j = 0$, i.e., if the jth zero lies on the positive real axis. According to Yang and Lee, zeros that come arbitrarily close to the real axis in the thermodynamic limit mark the transition points. This is essential for our study as we are interested here exclusively in transition properties of polymers of finite length. Therefore, we do not expect to find any real-valued zeros in the analysis of the complex-zero space of these systems. Rather, we will identify the zeros closest to the positive real axis which are called the leading zeros because they contribute most to the quantity of interest, if $x \approx a_j$. If such zeros have a rather isolated appearance in the distribution of the zeros in the complex map near the positive real axis, they represent a signal in that quantity that might become a singularity in the infinitely large system. At least, in the finite system, they indicate increased thermal activity. Canonical quantities such as the specific heat typically possess a peak or a "shoulder" in those regions in temperature space.

Technically, apart from finite-size scaling, there are two possibilities to define transition points for finite systems by means of partition function zeros. Either one considers the zero as if it lies on a circle (in first-order like transitions, the transition-state zeros distribute indeed near a circular line), in which case the radius defined via $|x_j|^2 = a_j^2 + b_j^2$ can be used to locate the intersection point on the positive real axis: $x_c \equiv a_j' = |x_j|$. Alternatively, since b_j will be small near the positive real axis, one can also simply choose $x_c = a_j \approx |x_j|$. Either way, by performing the projection upon the real axis, a specific-heat

singularity is mimicked *even for a finite system*. The transition point can then be defined by

$$T_{\rm c} = -\frac{\varepsilon}{k_{\rm B} \ln |x_j|}. \tag{8}$$

On this basis, conclusions about the structural transitions of finite-length flexible polymers will be drawn in this study, but these transitions should not be confused with the strictly defined thermodynamic phase transitions in the Yang-Lee sense.

The accurate estimation of the partition function zeros requires two separate parts that for a complex system can only be accomplished computationally. First, generalized-ensemble Monte Carlo simulations have to be performed to obtain the density of states. Second, all zeros of the polynomial form of the partition function must be identified. Since a polynomial of degree five or higher has no algebraic solution in general, as stated by the Abel-Ruffini theorem, the zeros can only be found by means of numerical computation. We will review the polymer model and the simulation and analysis methods used in the following.

B. Coarse-grained polymer model

A linear polymer of length L is formed by concatenation of L identical chemical units called monomers. Each monomer is composed of several atoms, thus the size of the chain suitable for simulation is limited by the computational resources and methods currently available. For the study of generic thermodynamic properties of polymers, however, all-atom models can typically be replaced by a simpler coarse-grained representation with effective interactions. We here consider such a generic coarse-grained model for linear, elastic, flexible polymers [16]. Non-bonded monomers interact pairwise via a truncated and shifted Lennard-Jones (LJ) potential

$$V_{\rm LJ}^{\rm mod}(r_{ij}) = V_{\rm LJ}(\min(r_{ij}, r_c)) - V_{\rm LJ}(r_c),$$

where r_{ij} denotes the distance between the ith and the jth monomer, r_c is the cutoff distance, and

$$V_{\rm LJ}(r) = 4\epsilon \left[\left(\frac{\sigma}{r}\right)^{12} - \left(\frac{\sigma}{r}\right)^{6} \right]$$

is the standard LJ potential. In this work the LJ parameters were chosen as $\epsilon = 1$, $\sigma = 2^{-1/6} r_0$, and $r_c = 2.5\sigma$.

The elastic bonds between monomers adjacent along the chain are modeled by the finitely extensible nonlinear elastic (FENE) potential [32]

$$V_{\rm FENE}(r_{ii+1}) = -\frac{K}{2} R^2 \ln \left[1 - \left(\frac{r_{ii+1} - r_0}{R} \right)^2 \right].$$

This potential possesses a minimum at r_0 and diverges for $r \to r_0 \pm R$. K is a spring constant and we set the parameters as $R = 0.3$, $r_0 = 0.7$, and $K = 40$.

C. Numerical methods

1. Monte Carlo sampling in a generalized ensemble

Since the simulation of structural phases of polymers is challenging, even for a coarse-grained model and moderate system sizes, a sophisticated advanced Monte Carlo update set [30] was applied in combination with multicanonical sampling [27, 28, 30]. The majority of moves consisted of attempted displacements of single monomers within a sphere around their original location. Depending on energy E and number of monomers N the radii of these spheres were chosen such that high acceptance rates could be achieved for all energies and system sizes. In addition, we used bond-rebridging moves, where all monomers keep their position, but the linkage between them is altered. Furthermore, a novel cut-and-paste move was developed in which one monomer is removed and reinserted in an entirely different location within the polymer chain.

Most of the data were produced in a single simulation by sampling a generalized "grand-multicanonical" ensemble [30]. The main goal was to avoid free energy barriers by enabling the system to change its size. Therefore, in addition to the trial update schemes described above, a Monte Carlo step was introduced by means of which single monomers could randomly be added or removed. A weight function $W(E, N)$ assured that all energies and sizes were visited with the same probability. It was tuned using a delayed Wang-Landau procedure, in which the modification factor of the original Wang-Landau method is made weight-dependent. If the multicanonical weight function at Monte Carlo "time" t is denoted by W_t, then it is modified after the next update to

$$W_{t+1}(E, N) = W_t(E, N) / f^{W_t(E,N)/W_{t-d}(E,N)} \tag{9}$$

for $E = E_{t-d}$, $N = N_{t-d}$. For other values of E and N, the weight remains unchanged as in a conventional multicanonical simulation. Therefore, the effect of the Wang-Landau modification factor f to smooth out the free-energy landscape is delayed by d. This slows down the saturation speed of Wang-Landau sampling and enables a better efficiency in exploring phase space regions of low entropy at low energy, in particular in isolated regions that might contain hidden barriers. For the polymer system considered here, this is particularly relevant in the solid-solid transition regime. A sufficiently large delay for the polymer model considered here is obtained by the choice $d = 10^4$.

Once the weights had converged data were generated in a grand-multicanonical production that consisted of approximately 2×10^{12} Monte Carlo moves and consumed about 0.5 CPU years.

2. Zeros finder

Computing the zeros of polynomials can be posed as an eigenvalue problem [33, 34]. Consider the matrix pair (**A**,**B**) where

$$\mathbf{A} = \begin{bmatrix} 0 & 0 & 0 & \cdots & 0 & -g_0 \\ 1 & 0 & 0 & \cdots & 0 & -g_1 \\ 0 & 1 & 0 & \cdots & 0 & -g_2 \\ 0 & 0 & 1 & \cdots & 0 & -g_3 \\ \vdots & \vdots & \vdots & \ddots & \vdots & \vdots \\ 0 & 0 & 0 & \cdots & 1 & -g_{n-1} \end{bmatrix} \tag{10}$$

is the Frobenius companion matrix related to a monic polynomial [35] of degree n [36], and

$$\mathbf{B} = \begin{bmatrix} 1 & 0 & 0 & \cdots & 0 & 0 \\ 0 & 1 & 0 & \cdots & 0 & 0 \\ 0 & 0 & 1 & \cdots & 0 & 0 \\ \vdots & \vdots & \vdots & \ddots & \vdots & \vdots \\ 0 & 0 & 0 & \cdots & 1 & 0 \\ 0 & 0 & 0 & \cdots & 0 & g_n \end{bmatrix}. \tag{11}$$

Then a straightforward computation shows that

$$\det\left(x\mathbf{B} - \mathbf{A}\right) = \sum_m g_m x^m = P(x). \tag{12}$$

On the other hand, the well-known generalized eigenvalue problem (GEP) [37] can be stated as

$$\det\left(\lambda\mathbf{B} - \mathbf{A}\right) = 0. \tag{13}$$

By comparing Eqns. (12) and (13) one finds that eigenvalues of the matrix pencil (**A**,**B**) are the zeros of P, i.e., $x_k = \lambda_k$. The GEP can be solved by the QZ algorithm [38], just after performing a balance on the matrix pair (**A**,**B**), which is very important for accuracy [39–41]. Both of these algorithms can be found in LAPACK [42]. Alternatively, as implemented in *Mathematica* [43], one can write a companion matrix of P as

$$\mathbf{C} = \begin{bmatrix} -g_1/g_0 & -g_2/g_0 & -g_3/g_0 & \cdots & -g_{n-1}/g_0 & -g_n/g_0 \\ 1 & 0 & 0 & \cdots & 0 & 0 \\ 0 & 1 & 0 & \cdots & 0 & 0 \\ 0 & 0 & 1 & \cdots & 0 & 0 \\ \vdots & \vdots & \vdots & \ddots & \vdots & \vdots \\ 0 & 0 & 0 & \cdots & 1 & 0 \end{bmatrix}. \tag{14}$$

Then the zeros of P are obtained directly by diagonalization of **C** and given by

$$x_k = \frac{1}{\lambda_k}. \tag{15}$$

This method is more time consuming but also more robust than the previous one.

We employed both methods for the estimation of the partition function zeros (3).

3. Microcanonical inflection-point analysis

An alternative approach to unravel transition properties of finite-size systems is the direct microcanonical analysis [19] of caloric quantities derived from the entropy $S(E) = k_{\mathrm{B}} \ln g(E)$. The basic idea is that the interplay of energy and entropy and, in particular, changes of it, signal cooperative system behavior that can be interpreted as a transition (and in the thermodynamic limit as a phase transition) of the system. Then first and higher derivatives of $S(E)$ reveal the transition points of the system in energy space. However, since the first derivative is the reciprocal microcanonical temperature,

$$\beta(E) \equiv T^{-1}(E) = \left(\frac{\partial S(E)}{\partial E}\right)_{N,V}, \tag{16}$$

energetic transition points can also be associated with transition temperatures. Transitions occur, if $\beta(E)$ responds least sensitively to changes in the energy. The slope of the corresponding inflection points can be used to distinguish first- and second-order transitions systematically. If

$$\gamma(E) = \left(\frac{\partial \beta(E)}{\partial E}\right)_{N,V} = \left(\frac{\partial^2 S(E)}{\partial E^2}\right)_{N,V} \tag{17}$$

exhibits a positive-valued peak at the inflection point, the transition resembles a first-order transition, whereas a negative-valued peak indicates a second-order transition. This method is called microcanonical inflection-point analysis [1]. In the following, we will compare the transition temperatures obtained from the leading zeros with microcanonical estimates.

III. RESULTS AND DISCUSSION

Based on the density of states estimates obtained in multicanonical simulations, we calculated the partition function zeros for the elastic flexible polymer model for chain lengths L ranging from 13 to 309 monomers. The structural transition behavior was investigated previously by conventional canonical statistical analysis of "peaks" and "shoulders" of fluctuating energetic and structural quantities as functions of the canonical temperature [16, 17]. Subsequently, the densities of states of this set of polymers were analyzed systematically by means of microcanonical inflection-point analysis, with particular focus on the typically hardly accessible low-temperature transition behavior (freezing, solid-solid transitions) [1]. The microcanonical analysis is based on estimates of the microcanonical entropy and *its derivatives*, and therefore requires highly accurate data. Therefore, it is not only interesting from the statistical physics point-of-view to study the partition function zeros, but also for practical purposes. The major information about structural transitions is already encoded in the corresponding leading zeros which are rather simple to identify. The partition function zero method thus turns out

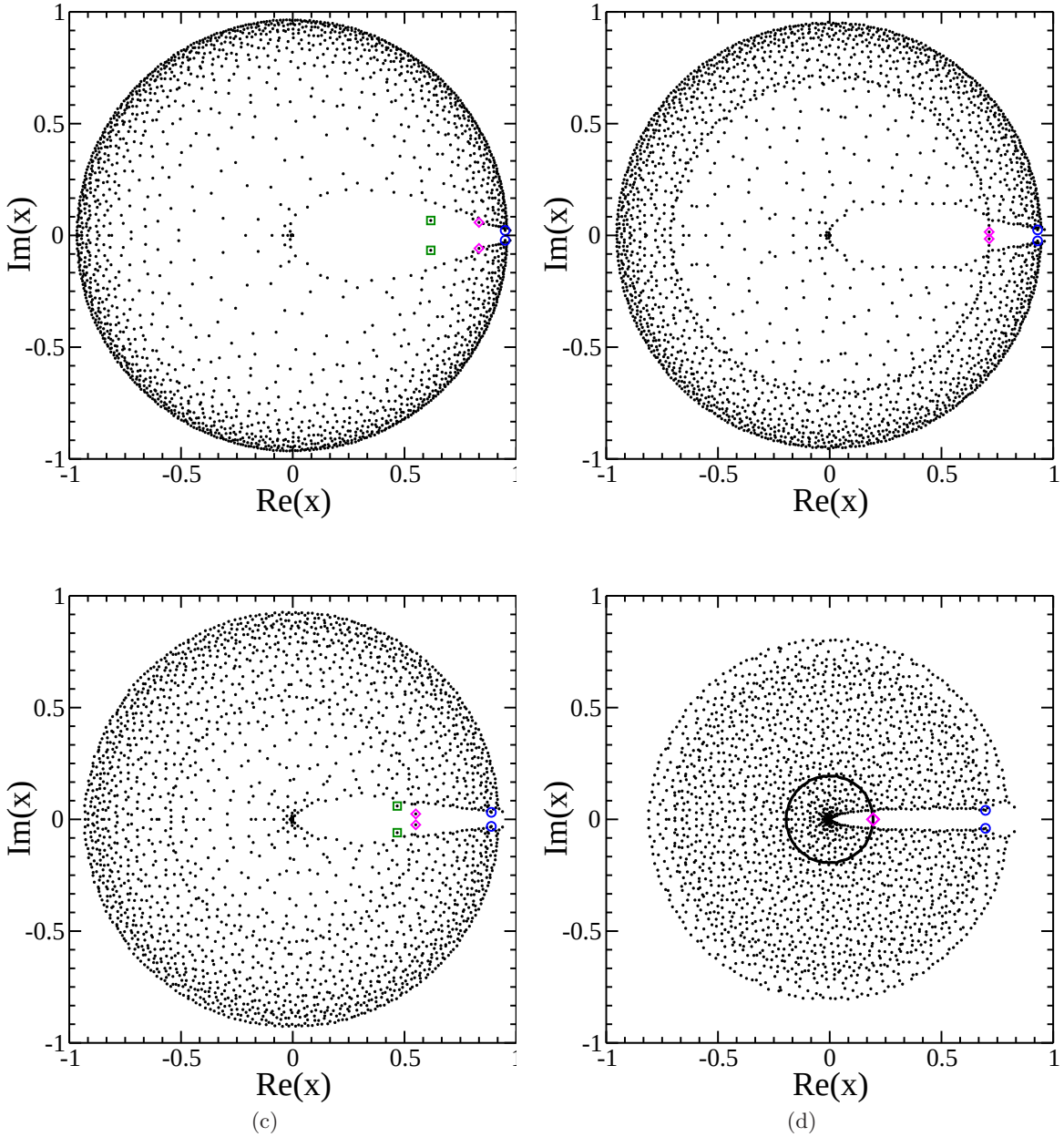

FIG. 2. Complex plane map of the partition function zeros for chain size: (a) $L = 35$, (b) $L = 55$, (c) $L = 90$, and (d) $L = 300$. The leading zeros are highlighted as follows: From $x = 0$ to 1 green squares denote "solid-solid" transitions, magenta diamonds denote "liquid-solid" transitions, and blue circles denote "gas-liquid" transitions.

to be a robust method for the identification of transition points. It is, therefore, highly interesting to verify whether this method is capable of finding indications for the same transitions that have already been identified by means of microcanonical inflection-point analysis.

Figure 2 shows the distributions of the zeros identified from the discretized densities of states for specific chain lengths $L = 35, 55, 90$, and 300 and using the energy bin sizes $\varepsilon = 0.07, 0.11, 0.20$, and 0.29, respectively. It is worth noting that the zeros, and thus their distribution, do generally depend on the choice of ε, but the transition temperature estimates remain widely unaffected if ε is changed. Moreover, since the data series used for the estimation of the density of states are finite, different simulation runs yield different values of the zeros.

Note that we plot the zeros differently than Ref. [14]. In our case they are strictly confined within a circle with radius 1 (the boundary at 1 corresponds to infinite temperature). We also define the transition temperature differently for a finite system. Ref. [14] considers only the real part of the leading zero, whereas we prefer the absolute value, motivated by the fact that at first-order transitions the zeros lie on a circle whose radius is a unique estimator for the transition temperature.

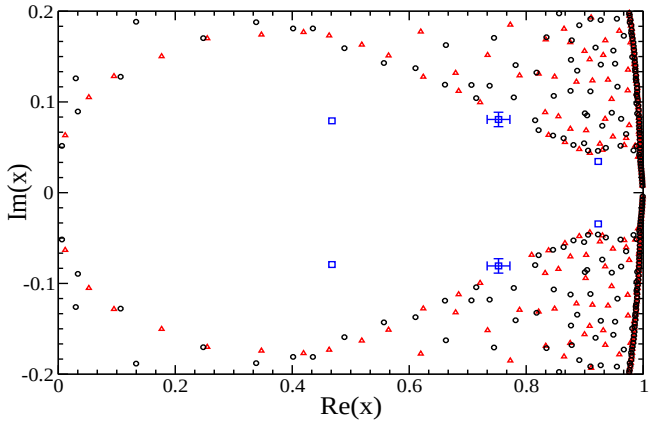

FIG. 3. Zoom into the zeros map for $L = 35$. Black circles and red triangles represent the zeros obtained in two different simulations. Whereas the positions of nonleading zeros vary, the leading zeros are very close to each other and the overall distribution pattern is very similar. The blue squares represent the average values of the leading zeros over ten different simulations. Error bars are shown for the leading zero that corresponds to the liquid-solid transition; in the other cases the error is smaller than the symbol size.

The section of the map for $L = 35$ shown in Fig. 3 contains sets of zeros obtained in two independent simulations (circles and triangles). By standard jackknife error analysis [44–48], the statistical error of the components of the complex zeros was estimated from ten independent simulations and error bars are shown for the leading zeros (squares) only (if larger than symbol size). Thus, for the analysis of transitions, the method is sufficiently robust and enables the identification of transition points.

We only analyze here the zero maps for $L = 35, 55, 90$, and 300, because these system sizes are representative for the various transition behaviors that have been systematically and uniquely identified for polymer chains with lengths in the above mentioned interval in canonical [16–18] and microcanonical analyses [1]. From these studies it is known that in this model polymers with "magic" length $L = 13, 55, 147, 309, \ldots$ possess a second-order-like collapse ("gas-liquid") transition and a very strong first-order-like freezing or "liquid-solid" transition from the compact, globular liquid phase into an almost perfect icosahedral Mackay structure [49], where the facets are arranged as fcc overlayers. For intermediate chain lengths, the optimal packing in the solid phase can be Mackay or anti-Mackay (hcp overlayers), depending on the system size and the temperature. In other words, for certain groups of chain lengths, an additional "solid-solid" transition can be found, in which anti-Mackay overlayers turn into energetically more preferred Mackay facets at very low temperatures [1, 16–18]. This behavior of finite particle systems is also well known from atomic clusters [50–53].

For the systems explicitly discussed here, this means that we expect to find three transitions for $L = 35$ and 90, whereas the solid-solid transition is absent for $L = 55$. For $L = 300$, the liquid-solid and the solid-solid transition merge and occur at about the same temperature. These transitions can be distinguished microcanonically, but not canonically. Therefore, we do not expect to find indications of separate transitions in the analysis of the leading zeros.

As earlier analyses revealed [1, 16], the liquid-solid and solid-solid transitions for system sizes $31 \leq L \leq 54$ have peculiar characteristics. Except for the special case $L = 38$ that forms a truncated fcc octahedron, these polymers crystallize in two different ways by cooling down from the liquid phase [16]. With high probability, more than one icosahedral nucleus crystallizes out of the liquid by forming anti-Mackay overlayers and by an additional solid-solid transition turns into a single icosahedral nucleus with 13 monomers and a Mackay overlayer formed by the remaining ones. Alternatively, with lower probability, the anti-Mackay multi-core structure can also form out of the liquid via an intermediate unstable phase dominated by a single-core structure with Mackay overlayer. Therefore, the anti-Mackay solid phase is a mixed phase that also contains Mackay morphologies. Therefore the liquid-solid transition for these system sizes does not exhibit the same characteristic as for larger polymers and is actually second-order-like [1]. To conclude, all three structural transitions for $L = 35$ are second-order-like. The corresponding zero maps shown in Figs. 2(a) and 3 indeed reveal three separate pairs of leading zeros that represent these transitions.

The polymer chain containing 55 monomers is "magic". For this reason, it exhibits a particularly strong liquid-solid transition at $T \approx 0.33$ into a perfect icosahedral conformation [16] with complete Mackay overlayer. A stable anti-Mackay phase does not exist and, therefore, no solid-solid transition occurs. Consequently, the zero map shown in Fig. 2(b) reveals only two sets of leading zeros representing the Θ collapse and the nucleation transition. The most striking feature is the observation that there is an increased accumulation of zeros on a circle that contains the pair of the leading zeros associated with the liquid-solid transition. The circular distribution has to be attributed to the self-reciprocity of the partition function polynomial [54] at a phase transition with coexisting phases in which case the energetic canonical distribution is bimodal and virtually symmetric. Therefore, the circular pattern can be interpreted as the signature of first-order-like transitions in the map of Fisher partition function zeros.

For the polymer with $L = 90$ monomers, the structural transitions can clearly be identified in the corresponding zeros map [Fig. 2(c)]. The liquid-solid transition into the anti-Mackay solid phase is represented by a circular zeros distribution, but neither the collapse transition nor the solid-solid crossover to icosahedral Mackay structures exhibit obvious features in the zero distribution other than prominent locations of the leading zeros. In correspondence with the previous microcanonical analysis, these

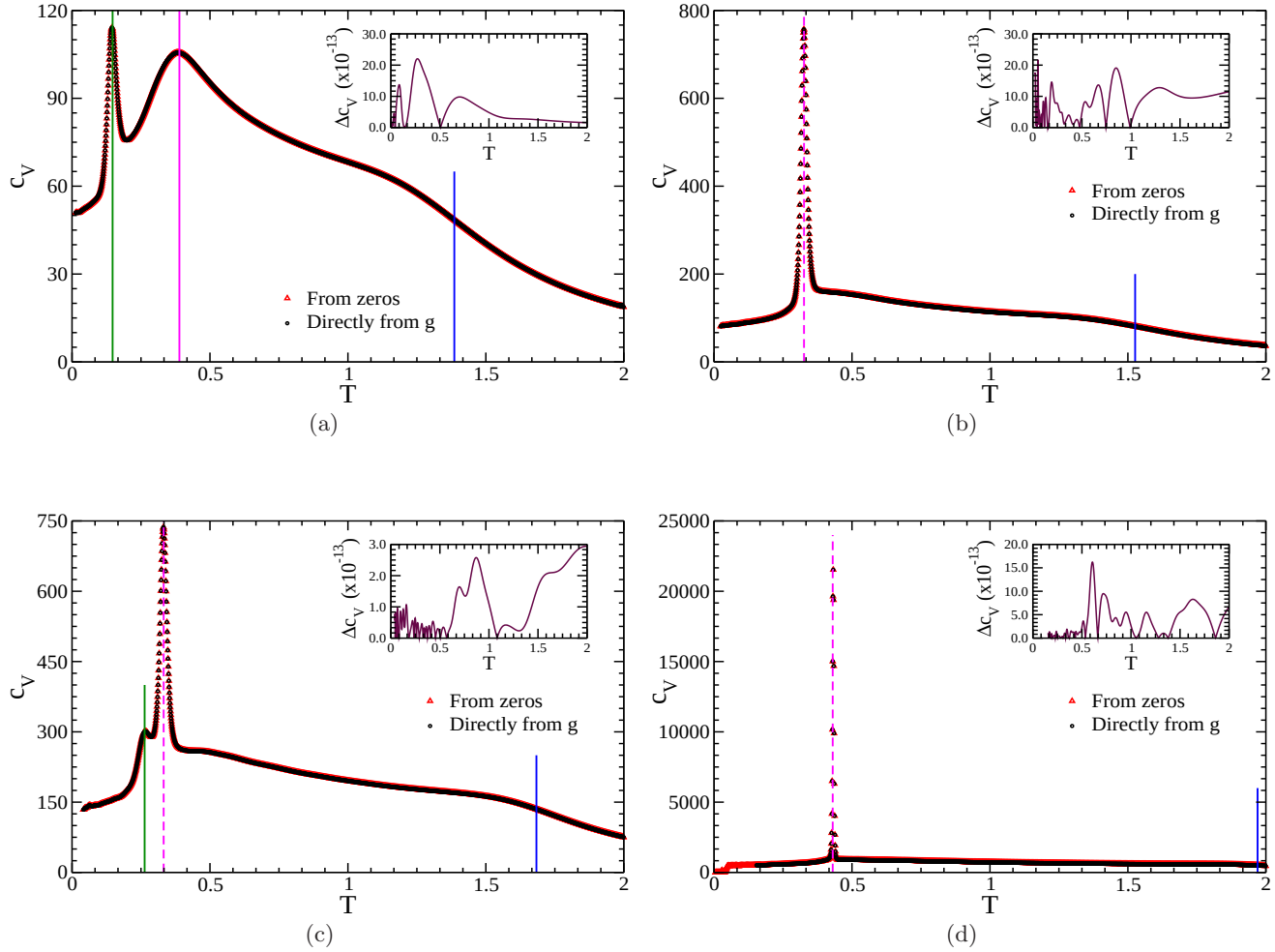

FIG. 4. Heat capacity curves for chain sizes: (a) $L = 35$, (b) $L = 55$, (c) $L = 90$, and (d) $L = 300$. Plotted are the curves obtained from the zeros of the partition function and, for comparison, by direct calculation from the density of states. The inset shows the relative differences between them. The small deviations make it evident that all zeros were identified correctly. The vertical lines are located at the transition temperatures calculated from the leading zeros. Dashed and solid lines represent first- and second-order-like transitions, respectively.

transitions are classified as of second order. It is worth mentioning that the chain length $L = 90$ is close to the threshold length ($L \approx 110$), at which in the canonical interpretation the liquid turns directly to solid Mackay structures at the liquid-solid transition point and liquid-solid and solid-solid transitions merge.

No separate solid-solid transition occurs for chain lengths $L > 110$ until the next "magic" limit $L = 147$ is reached [1, 17], i.e., the Mackay phase is the only stable solid phase. Microcanonically speaking, the solid-solid transition lies energetically within the latent heat interval of the first-order liquid-solid transition and can no longer be resolved in the canonical analysis (the specific heat exhibits only one sharp peak in these cases [17]). The zeros map shown in Fig. 2(c) reveals a very pronounced circular distribution and the projected intersection point with the positive x axis corresponds indeed to the liquid-solid transition temperature.

While $L = 90$ is a length *below* the anti-Mackay–Mackay threshold, our last example $L = 300$, is above the corresponding threshold in the following segment of chain lengths that lies between two magic lengths, $147 < L \leq 309$ ($L = 309$ is the next "magic" chain length). The most surprising feature is that in temperature space liquid-solid and solid-solid transitions merge, whereas energetically both can be distinguished clearly as first-order-like transitions [1]. The trend is that the solid-solid transition will shift to *higher* microcanonical temperatures than the liquid-solid transition when increasing L towards $L = 309$. This microcanonical crossover behavior has already been known in other systems and is a pure finite-size effect [26]. The corresponding root map shown in Fig. 2(d) displays only the general canonical behavior; therefore, only one circle represents this first-order-like double-transition.

For the explicit estimation of the transition temperatures from the Fisher zeros according to Eq. (8), there is the ambiguity to use either the absolute values of the

TABLE I. Comparison of transition temperatures for solid-solid (ss), liquid-solid (ls), and gas-liquid (gl) transitions for $L = 35, 55, 90$, and 300 as obtained by the partition function zero method ($T_{\rm z}$) and by microcanonical inflection-point analysis ($T_{\rm m}$). These estimates are compared to peak positions of the heat-capacity curves ($T_{c_V}^{\rm ss,ls}$) and fluctuations of the radius of gyration ($T_{d\langle R\rangle/dT}^{\rm gl}$), respectively. The maximum 1σ tolerance of all estimates is ± 1 in the last digit. There is no solid-solid transition for the 55-mer. The solid-solid transition of the 300-mer can only be distinguished from the liquid-solid transition in the microcanonical inflection-point analysis.

	solid-solid			liquid-solid			gas-liquid		
L	$T_{\rm z}^{\rm ss}$	$T_{\rm m}^{\rm ss}$	$T_{C_V}^{\rm ss}$	$T_{\rm z}^{\rm ls}$	$T_{\rm m}^{\rm ls}$	$T_{C_V}^{\rm ls}$	$T_{\rm z}^{\rm gl}$	$T_{\rm m}^{\rm gl}$	$T_{d\langle R\rangle/dT}^{\rm gl}$
35	0.15	0.14	0.14	0.39	0.39	0.38	1.39	1.39	1.35
55	N/A	N/A	N/A	0.33	0.33	0.33	1.53	1.51	1.53
90	0.26	0.26	0.27	0.33	0.33	0.33	1.68	1.65	1.67
300	N/A	0.44	N/A	0.43	0.43	0.43	1.97	1.88	1.97

complex zeros or their real parts only,

$$T_{\rm tr} = -\frac{2\varepsilon}{k_{\rm B}\ln\left(a_j^2+b_j^2\right)} \approx -\frac{\varepsilon}{k_{\rm B}\ln a_j}. \qquad (18)$$

Both values differ for finite systems, but converge in the thermodynamic limit. Since we already know that distributions of zeros for first-order-like transitions are circular, we chose to define transition points by means of the absolute values (corresponding to the radius of the circle). For the four examples that we discuss here in more detail, the corresponding values are listed in Table I. These estimates are in very good agreement with the transition temperatures obtained by microcanonical analysis. Since the Θ transition is only represented by a weak shoulder in the heat capacity curves shown in Fig. 4, we consider in these cases the corresponding peak positions of the fluctuations of the radius of gyration, $d\langle R_{\rm gyr}\rangle/dT$ as a more appropriate indicator of these transitions. This is a general problem of the canonical analysis of fluctuating quantities and the major reason for the introduction of methods that enable a unique identification of transition points even for finite systems.

For this reason both the zeros method and the microcanonical inflection-point analysis are more useful for the definition of unique transition temperatures than the conventional approach of the quantitative analysis of fluctuating quantities. Furthermore, the analysis of zero distributions or microcanonical inflection points allow the discrimination between first- and second-order-like transitions. This information is not easily accessible from ordinary canonical statistical analysis. In Figs. 4(a)- 4(d), vertical lines are located at the positions of the transition transitions obtained by the analysis of the Fisher zeros.

Fig. 5 summarizes our results of the Fisher zero analysis for all chain lengths in the interval $13 \le L \le 309$. For comparison, the data from the microcanonical inflection-point analysis are also shown. Although basically founded on the conventional canonical understanding of temperature, the zeros method captures surprisingly many details of transition behavior in finite polymer systems that were formerly accessible only by microcanonical analysis. Note that the temperature axis represents the microcanonical transition temperatures in the case of the microcanonical analysis, whereas it scales canonical transition temperatures obtained by the zeros method. These temperature estimates do not typically coincide, and this is why larger deviations in the estimates of transition temperatures seem to occur, particularly for small systems. Furthermore, in those cases the indicators for the transitions are very weak (which means that the transitions are also very weak) in both methods. This explains why the numerical error of the transition temperatures is larger for small systems than it is for larger ones ($L \ge 55$) that exhibit more stable structural phases.

IV. SUMMARY

We calculated Fisher partition function zeros for a generic model of flexible, elastic polymers on the basis of accurate estimates of the densities of states for chain

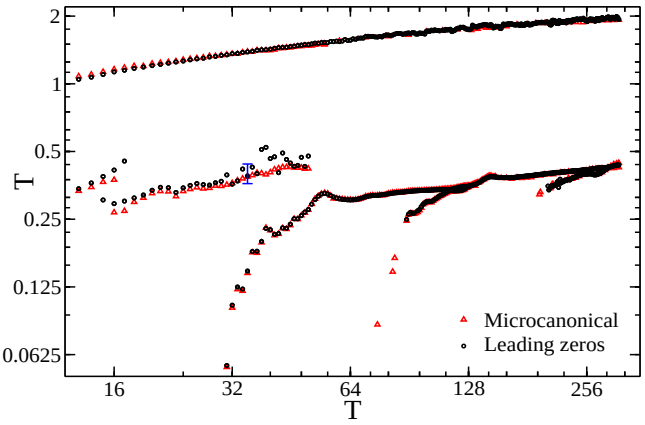

FIG. 5. Transition temperatures of conformational transitions for elastic, flexible polymers with chain lengths ranging from $L = 13$ to 309. The black dots represent the transition temperatures obtained from the leading zeros of the partition function. For comparison, the transition temperatures obtained by microcanonical inflection-point analysis are also shown (red triangles).

lengths $13 \leq L \leq 309$. For there entire range of chain lengths, we estimated transition temperatures systematically by analyzing the leading zeros and their distributions. We identified the gas-liquid and liquid-solid transition points, as well as the notoriously difficult to find solid-solid transitions, which are only surface effects but nonetheless relevant for finite systems. Our estimates of transition temperatures are in very good agreement with formerly obtained results by microcanonical inflection-point analysis for the same model [1]. By comparison with the microcanonical classification scheme, we found numerical evidence for the circular pattern of the zeros associated with coexisting states in first-order-like transitions. Because the zeros method is capable of revealing these signals, we conclude on the basis of the results of our study that this method can be used for the identification of transitions in small systems as well; otherwise it would have had to be abandoned for this purpose.

We find that both the microcanonical inflection-point analysis and the Fisher zeros method enable a quantitative analysis of all "transitions" of a finite system. Both methods strongly outperform the conventional canonical approach of analyzing the "peak-and-shoulder" characteristics of thermodynamic quantities such as the specific heat or canonical fluctuations of order parameters as functions of the heat bath temperature. Whereas microcanonical analysis enables a more fine-tuned understanding of an individual transition (such as the composition of subphase transitions), the zeros method is very robust and the leading zeros are less sensitive to numerical errors. This remarkable robustness can be attributed to the fact that the leading zeros alone govern in all thermodynamic quantities the ultimate approach to the transition point in the scale-free, universal regime. Numerical errors can be interpreted as perturbations of the model, but such effective model details have hardly any impact on the thermodynamic behavior of the system near a transition point, even for relatively small systems. This is not the case within the phases, where the location of the zeros depends more sensitively on details.

ACKNOWLEDGMENTS

We would like to thank Shan-ho Tsai, Lucas A. S. Mól, and Bismarck V. Costa for inspiring discussions. JCSR thanks CNPq (National Council for Scientific and Technological Development, Brazil) for the support under grant No. PDE 202122/2011-5. MB acknowledges partial support of this project by the NSF under Grant No. DMR-1207437 and by CNPq under Grant No. 402091/2012-4.

[1] S. Schnabel, D. T. Seaton, D. P. Landau, and M. Bachmann, Phys. Rev. E **84**, 011127 (2011).
[2] P. Ehrenfest and T. Ehrenfest, *The Conceptual Foundation of the Statistical Approach in Mechanics* (Cornell University Press, Ithaca NY, 1959), reprint of the German 1912 edition.
[3] L. D. Landau, Nature **138**, 840 (1936).
[4] M. E. Fisher, Rep. Prog. Phys. **30**, 615 (1967).
[5] L. P. Kadanoff, W. Götze, D. Hamblen, R. Hecht, E. A. S. Lewis, V. V. Palciauskas, M. Rayl, J. Swift, D. Aspnes, and J. Kane, Rev. Mod. Phys. **39**, 395 (1967).
[6] P. Heller, Rep. Prog. Phys. **30**, 731 (1967).
[7] C. N. Yang and T. D. Lee, Phys. Rev. **87**, 404 (1952); T. D. Lee and C. N. Yang, Phys. Rev. **87**, 410 (1952).
[8] M. E. Fisher, in *Lectures in Theoretical Physics vol. 7C*, ed. by W. E. Brittin (University of Colorado Press, Boulder, 1965), Chap. 1.
[9] W. Janke and R. Kenna, J. Stat. Phys. **102**, 1211 (2001); Comp. Phys. Comm. **147**, 443 (2002); Nucl. Phys. B (Proc. Suppl.) **106-107**, 905 (2002).
[10] C.-O. Hwang, Phys. Rev. E **80**, 042103 (2009).
[11] J. S. M. Fonseca, L. G. Rizzi, and N. A. Alves, Phys. Rev. E **86**, 011103 (2012).
[12] N. A. Alves and U. H. E. Hansmann, Phys. Rev. Lett. **84**, 1836 (2000).
[13] J. Wang and W. Wang, J. Chem. Phys. **118**, 2952 (2003).
[14] M. P. Taylor, P. P. Aung, and W. Paul, Phys. Rev. E **88**, 012604 (2013).
[15] C.-N. Chen, Y.-H. Hsieh, and C.-K. Hu, EPL **104**, 20005 (2013).
[16] S. Schnabel, T. Vogel, M. Bachmann, and W. Janke, Chem. Phys. Lett. **476**, 201 (2009).
[17] S. Schnabel, M. Bachmann, and W. Janke, J. Chem. Phys. **131**, 124904 (2009).
[18] D. T. Seaton, T. Wüst, and D. P. Landau, Phys. Rev. E **81**, 011802 (2010).
[19] D. H. E. Gross, *Microcanonical Thermodynamics* (World Scientific, Singapore, 2001).
[20] T. Chen, X. Lin, Y. Liu, H. Liang, Phys. Rev. E **76** 046110 (2007).
[21] M. P. Taylor, W. Paul, and K. Binder, J. Chem. Phys. **131**, 114907 (2009); Phys. Rev. E **79**, 050801(R) (2009).
[22] M. Bachmann, Phys. Proc. **3**, 1387 (2010).
[23] C. Junghans, M. Bachmann, and W. Janke, Phys. Rev. Lett. **97**, 218103 (2006); J. Chem. Phys. **128**, 085103 (2008); Europhys. Lett. **87**, 40002 (2009).
[24] L. Wang, T. Chen, X. Lin, Y. Liu, H. Liang, J. Chem. Phys. **131**, 244902 (2009).
[25] M. Möddel, W. Janke, and M. Bachmann, PhysChemChemPhys **12**, 11548 (2010).
[26] J. Gross, T. Neuhaus, T. Vogel, and M. Bachmann, J. Chem. Phys. **138**, 074905 (2013).
[27] B. A. Berg and T. Neuhaus, Phys. Lett. B **267**, 249 (1991); Phys. Rev. Lett. **68**, 9 (1992).
[28] W. Janke, Physica A **254**, 164 (1998); B. A. Berg, Comp. Phys. Commun. **153**, 397 (2003); M. Bachmann, Phys. Scr. **87**, 058504 (2013).
[29] F. Wang and D. P. Landau, Phys. Rev. Lett. **86**, 2050 (2001); Phys. Rev. E **64**, 056101 (2001); D. P. Landau, S.-H. Tsai, and M. Exler, Am. J. Phys. **72**, 1294 (2004).
[30] S. Schnabel, W. Janke, and M. Bachmann, J. Comput. Phys. **230**, 4454 (2011).

[31] T. Vogel, M. Bachmann, and W. Janke, Phys. Rev. E **76**, 061803 (2007).

[32] R. B. Bird, C. F. Curtiss, R. C. Armstrong, and O. Hassager, *Dynamics of Polymeric Liquids*, 2nd ed. (Wiley, New York, 1987); K. Kremer and G. S. Grest, J. Chem. Phys. **92**, 5057 (1990); A. Milchev, A. Bhattacharaya, and K. Binder, Macromolecules **34**, 1881 (2001).

[33] P. Van Dooren and P. Dewilde, Lin. Alg. Appl. **50**, 545 (1983).

[34] W. H. Press, S. A. Teukolsky, W. T. Vetterling, and B. P. Flannery, *Numerical Recipes in Fortran 77: The Art of Scientific Computing*, 2nd ed. (Cambridge University Press, New York, 1992), Chap. 9.5.

[35] In a monic polynomial of degree n, the nth coefficient is unity, i.e., $g_n = 1$.

[36] H. Linden, Lin. Alg. Appl. **271**, 41 (1998).

[37] D. S. Watkins, "The Generalized Eigenvalue Problem", in *The Matrix Eigenvalue Problem* (SIAM, 2007), p. 233.

[38] C. Moler and G. Stewart, SIAM J. Numer. Anal. **10**, 241 (1973).

[39] B. Parlett and C. Reinsch, Numer. Math. **13**, 293 (1969).

[40] R. Ward, SIAM J. Sci. Stat. Comp. **2**, 141 (1981).

[41] D. Lemonnier and P. Van Dooren, SIAM J. Matrix Anal. Appl. **28**, 253 (2006).

[42] www.netlib.org/lapack

[43] E. W. Weisstein, "Polynomial roots", in *MathWorld – A Wolfram Web Resource*, `http://mathworld.wolfram.com/PolynomialRoots.html`.

[44] R. G. Miller, Biometrika **61**, 1 (1974).

[45] B. Efron, *The Jackknife, the Bootstrap, and Other Resampling Plans* (SIAM, Philadelphia, 1982).

[46] W. Janke, "Statistical Analysis of Simulations: Data Correlations and Error Estimation", in *Proceedings of the Winter School "Quantum Simulations of Complex Many-Body Systems: From Theory to Algorithms"*, John von Neumann Institute for Computing, Jülich, NIC Series vol. **10**, ed. by J. Grotendorst, D. Marx, and A. Muramatsu (NIC, Jülich, 2002), p. 423.

[47] D. P. Landau and K. Binder, *A Guide to Monte Carlo Simulations in Statistical Physics*, 4th ed. (Cambridge University Press, New York, 2014), in press.

[48] M. Bachmann, *Thermodynamics and Statistical Mechanics of Macromolecular Systems* (Cambridge University Press, New York, 2014).

[49] A. L. Mackay, Acta Crystallogr. **15**, 916 (1962).

[50] J. A. Northby, J. Chem. Phys. **87**, 6166 (1987).

[51] D. J. Wales and J. P. K. Doye, J. Phys. Chem. A **101**, 5111 (1997).

[52] E. G. Noya and J. P. K. Doye, J. Chem. Phys. **124**, 104503 (2006).

[53] P. A. Frantsuzov and V. A. Mandelshtam, Phys. Rev. E **72**, 037102 (2005).

[54] W. Chen, J. Math. Anal. Appl. **190**, 714 (1995).